VIII
1973
москва

PROCEEDINGS OF THE EIGHTH INTERNATIONAL CONFERENCE ON SOIL MECHANICS AND FOUNDATION ENGINEERING

ТРУДЫ ВОСЬМОГО МЕЖДУНАРОДНОГО КОНГРЕССА ПО МЕХАНИКЕ ГРУНТОВ И ФУНДАМЕНТОСТРОЕНИЮ

COMPTES RENDUS DU HUITIEME CONGRES INTERNATIONAL DE MECANIQUE DES SOLS ET DES TRAVAUX DE FONDATIONS

1.2

VIII

1973

москва

PROCEEDINGS OF THE EIGHTH INTERNATIONAL CONFERENCE ON SOIL MECHANICS AND FOUNDATION ENGINEERING

ТРУДЫ ВОСЬМОГО МЕЖДУНАРОДНОГО КОНГРЕССА ПО МЕХАНИКЕ ГРУНТОВ И ФУНДАМЕНТОСТРОЕНИЮ

COMPTES RENDUS DU HUITIEME CONGRES INTERNATIONAL DE MECANIQUE DES SOLS ET DES TRAVAUX DE FONDATIONS

Contents

Table des Matières

Оглавление

A TRUE TRIAXIAL APPARATUS TO TEST ROCKFILLS

UN APPAREIL VRAIMENT TRIAXIAL POUR L'ESSAI DES ENROCHEMENTS
УСТАНОВКА ТРЕХОСНОГО СЖАТИЯ ДЛЯ ИСПЫТАНИЯ КАМЕННОЙ НАБРОСКИ

RAUL J. MARSAL, Research Professor of the Instituto de Ingenieria, (UNAM) and Advisor of the Comision Federal de Electricidad (CFE), Mexico

SYNOPSIS. The paper briefly deals with a statistical theory through which the frictional resistance inside a granular material is evaluated. By using the above mechanical concept, incremental stress-strain laws are proposed. This theoretical introduction is followed by the description of an apparatus that has been built at the Instituto de Ingeniería (UNAM), to perform "true" triaxial tests in which the ratio of the three principal stresses can be controlled at will. Emphasis is placed on the instrumentation and the means to apply uniform normal stresses to the specimen. The types of test to be carried out in the future are discussed.

INTRODUCTION

One of the most pressing problems of Soil Mechanics, is the search for the basic stress-deformation laws of soils. Up to present, engineers have used linear or hyperbolic relationships (Kondner and Zelasko, 1963) based mainly on results of triaxial compression tests. Both approaches have been found acceptable in some special cases, but it is recognized that they do not constitute a correct answer to the more general problems frequently found in engineering. For instance, the differences between the computed stresses and strains and the field measurements for the first filling of a rockfill dam, are far from negligible (Alberro, 1971).

Serious efforts have been made recently to better understand the basic laws, both through theory and experimental work (Reséndiz, 1970). In Mexico, the construction of high earth and rockfill dams has advanced the state of the art of the instrumentation of these structures to observe their behavior and also has stimulated the investigation of the strength and compressibility of granular materials (Marsal and Ramírez de Arellano, 1967; Marsal et al, 1965). The last stage of this field-laboratory research program undertaken by the Instituto de Ingeniería (UNAM) and the Comisión Federal de Electricidad (CFE), is directed to the study of the stress-deformation characteristics of particulate masses. To this end, the true triaxial apparatus described further was designed and built.

THEORETICAL FRAME

A statistical theory was proposed (Marsal, 1971), with the main purpose of assessing the frictional resistance that generates inside a granular soil. This model is founded on several principles and simplifying assumptions, which are briefly reviewed. In addition, the distribution of contact forces, the expression of the frictional resistance, and the incremental laws of deformation are presented.

Basic principles. The stresses acting on a particulate mass develop contact forces between the grains, P_{ij} (Fig. 1a). The magnitude and orientation of these forces depend on 1) the dimensions and shape of the particles*, 2) the mechanical properties of the rock grains and 3) the particle arrangement in the vicinity of each contact. The effect of the above factors on P_{ij} cannot be evaluated in a deterministic manner; furthermore, the analysis of P_{ij} based on the equilibrium equations suggests that the contact force components on a cartesian frame may be treated as random variables.

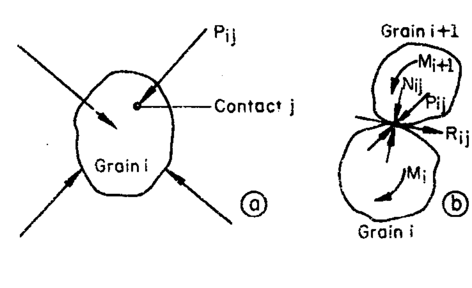

Fig. 1 Contact and friction forces

* Particles and grains are synonymous in this paper.

The shear strength is the result of friction forces (R_{ij}) produced at the contacts by both the normal components of P_{ij} and the grain moments (Fig. 1b). Friction forces have the direction of the relative movements between the particles, and in average, they are parallel to the mean path of the grains; the direction of this path can be determined with the strain theory of the continuum mechanics (Marsal, 1971).

It is postulated that the strain increment ($\Delta\varepsilon$) is proportional to the effective stress increment ($\Delta\rho$) applied to the mass divided by its available frictional resistance (r)*, all measured on the same direction.

$$\Delta\varepsilon = a\,\frac{\Delta\rho}{r} \tag{1}$$

When $\Delta\rho$ is the normal stress increment $\Delta\sigma_z$, it also causes a deformation perpendicular to the direction z which is proportional to $\Delta\sigma_z$. Shear stresses ($\Delta\rho = \Delta\tau$) are associated with shear strains only. It is acceptable to add strain increments, produced either by normal or shear stresses, or both, provided they are small.

Main hypotheses. The rockfill material is homogeneous in the sense that it has the same granulometric composition in any element of the mass; rock grains may be different in size but randomly distributed. It is assumed that the particles are spheres with diameters given by the grain-size curve of the soil; to partially correct the effect of this idealization a shape factor is used (Marsal, 1963).

The probability that a plane θ passed through the soil intersects a grain at any height (h_i) is constant (Fig. 2a). In addition, the number of contacts over the grain caps (n_{ci}) detached by plane θ is a random, discrete variable of constant density (Fig. 2b).

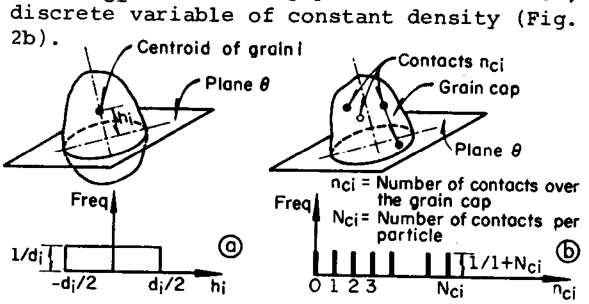

Fig. 2 Probabilistic distribution of h_i and n_{ci}

* The available resistance is equal to the frictional resistance minus the shear stress in the plane parallel to the mean path of the particles.

The total load transmitted across the plane θ is distributed among the grains in proportion to the cross-sectional areas intersected by plane θ. Furthermore, it is assumed that the coefficient of variation of the P_{ij}-component forces depends on the grain-size distribution and the effective stresses (Marsal, 1971).

The sliding friction forces at the grain contacts are proportional to the normal components of P_{ij}; the constant of proportionality is the coefficient of interparticle friction (μ_{ij}).

Contact forces. Based on the above assumptions, the component forces of P_{ij} on a cartesian frame (x, y, z) approach asymptotically functions of normal type (Central Limit Theorem); the average magnitude of P_{ij} and the standard deviations of components P_{xij}, P_{yij} and P_{zij}, for any plane θ, are:

$$\bar{P} = \frac{2\,\chi\,p}{\bar{N}_c\, n_s} \tag{2}$$

$$D(P_{xij}) = \frac{\tau_{zx}}{n_s}\sqrt{\frac{2}{\bar{N}_c}\left|v^2(A) + \left(\frac{n_s Q}{\tau_{zx}}\right)^2 - \frac{1}{3}\right|} \tag{3}$$

in which p=resultant stress ($= \sqrt{\tau_{zx}^2+\tau_{zy}^2+\sigma_z^2}$); τ_{zx}, τ_{zy} and σ_z = shear and effective normal stresses for plane θ ; $\bar{N}_c$ = mean number of contacts per particle; n_s = number of grains cut by plane θ , per unit of area; χ = coefficient that accounts for the probabilistic distribution of P_{ij}; $v^2(A)$ = variance of intersected grain areas; and Q=soil parameter related to soil gradation and its compaction. To obtain expressions $v(P_{yij})$ and $v(P_{zij})$ change in Eq. 3 τ_{zx} by τ_{zy} and σ_z, respectively.

The frequency function of the intensities of P_{ij} forces is presented in Fig. 3

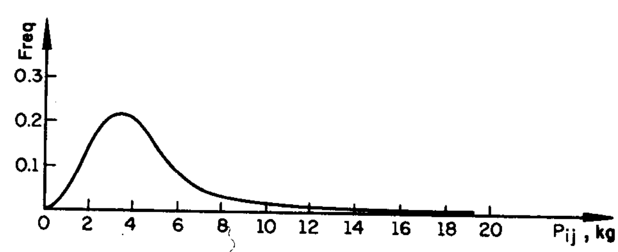

Fig. 3 Statistical distribution of P_{ij} intensities

Frictional resistance. The frictional resistance can be represented by a vector that has the direction of the mean path of the grains and a magnitude s equal to the difference of the sliding resistance s_n and the rolling stress t_m (Marsal, 1971),

$$s = s_n - t_m = fp - m\tau \qquad (4)$$

where p and τ are the resultant and shear stresses for the plane θ parallel to the mean path of the particles, and

$$f = \frac{b\,\chi\,\bar{\mu}\,\Sigma}{\sqrt{1+\bar{\mu}^2}}, \quad m = \frac{c}{\sqrt{12}} \qquad (5,6)$$

In the above formuli, b = b'b", in which b' is the average value of cos β_{ij} (Fig. 4) and b", is the number of contacts on plane θ ; $\bar{\mu}$ =mathematical expectation of the interparticle friction μ_{ij}; χ =coefficient related to the statistical distribution of P_{ij}; Σ =factor that depends on the grain-size distribution and the number of contacts per particle; and c=parameter that reflects the shape of grains, its value being in the interval 0-1.

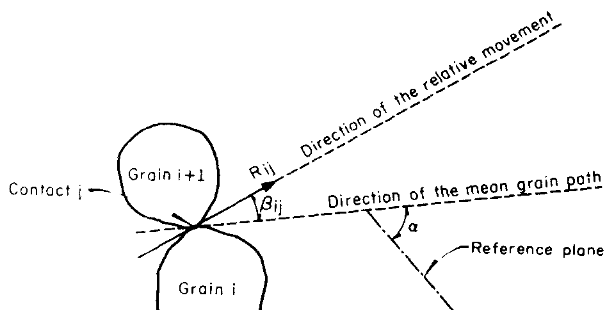

Fig. 4 Sliding friction forces

Fig. 5 shows the variation of the frictional resistance (s), the shear stress (τ), and the inclination of the mean path of the grains (θ) for a specimen tested in triaxial compression, in terms of the axial strain (ε_a). Near the origin (ε_a=0), the frictional resistance may increase appreciably due to effect of the standard deviation of P_{ij}-components (Eq. 3) on the coefficient χ of Eq. 5.

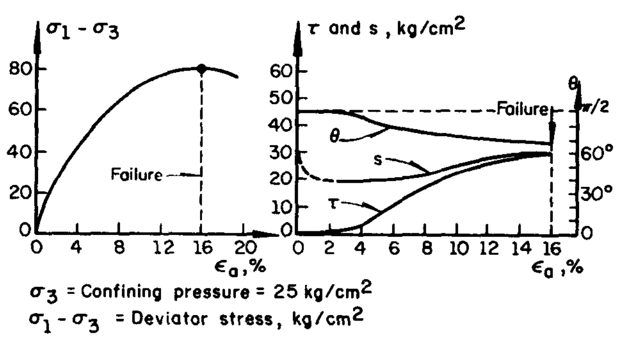

Fig. 5 Frictional resistance in a granular material tested under triaxial compression

Incremental laws. Bearing in mind Eq. 1 and assuming that the applied effective stresses are normal only, the stress-strain relationship for direction x is:

$$\Delta\varepsilon_x = a_n \frac{\Delta\sigma_x - \kappa(\Delta\sigma_y + \Delta\sigma_z)}{(s-\tau)\cos\alpha_x} \qquad (7)$$

where $\Delta\sigma_x$, $\Delta\sigma_y$ and $\Delta\sigma_z$ = increments of normal stresses for three orthogonal axes; $(s-\tau)$ = available frictional resistance on the plane parallel to the mean path of the particles; cos α_x = director cosine of the mean path of the grains; κ and a_n = dimensionless coefficients. The expressions for the other directions y and z, are obtained by proper change of the subindexes. In general the available resistance components have different magnitudes. Therefore, a granular soil is inherently anisotropic.

By considerations similar to those made in the preceding case, the incremental equations for shear stresses can be established. They are not presented here because of space limitations.

Implications of the theory. If the incremental laws for normal stresses (Eq. 7 and similar ones for y and z directions) are applied to a hydrostatic compression test, one obtains:

$$\Delta\varepsilon = a_n \frac{\sqrt{3}\,(1-2\kappa)}{f}\frac{\Delta\sigma}{\sigma}, \quad \sigma > \sigma_0 \qquad (8)$$

This is the well known logarithmic function found by testing; σ_0 depends on the granulometric composition of the material and its compaction. Within the interval $0 \leqslant \sigma \leqslant \sigma_0$, deformations $\Delta\varepsilon$ are small and approximately their relationship with σ is linear.

In a triaxial compression test, the expressions for the axial and radial strain increments ($\Delta\varepsilon_a$ and $\Delta\varepsilon_r$), result:

$$\Delta\varepsilon_a = \frac{\Delta\sigma_a}{(s-\tau)\sin\theta}, \quad \Delta\varepsilon_r = -a_n\frac{\kappa\,\Delta\sigma_a}{(s-\tau)\cos\theta}, \quad \theta < \frac{\pi}{2} \qquad (9,10)$$

in which θ = angle of inclination of the mean path of the grains relative to the major principal plane; and $\Delta\sigma_a$ = the increment of axial stress. Eq. 10 is indeterminate for σ_a -values close to the origin, because both κ and cos θ tend to zero. The modulus of deformation,

$$M_{TC} = \frac{(s-\tau)\sin\theta}{a_n} \qquad (11)$$

decreases with the available resistance and becomes zero when the frictional resistance s is equal to the shear stress τ acting on plane θ (Fig. 5). According to the theory (Marsal, 1971), this implies failure and from Eq. 4 the corresponding ratio of shear and normal stresses is:

$$(\frac{\tau}{\sigma})_{fail.} = \frac{f}{\sqrt{(1+m)^2 - f^2}} \tag{12}$$

By inspecting Eqs. 5 and 6, one can foresee the effects of 1) the interparticle friction, 2) the shape of the particles and 3) the statistical distributions of both contact forces and coefficients μ_{ij}, on the failure of a granular mass. In addition, $f \leqslant (1+m) \leqslant 1.29$, since $c \leqslant 1$ in Eq. 6.

The relationship between κ and K_o is theoretically found by applying Eq. 7 to the radial component $\Delta\varepsilon_r$ of a K_o- triaxial test. Then,

$$\Delta\varepsilon_x = a_n \frac{\Delta\sigma_x - \kappa(\Delta\sigma_y + \Delta\sigma_z)}{(s-\tau)\cos\alpha_x} \tag{13}$$

in which $\Delta\sigma_x$ and $\Delta\sigma_z$ are the radial and axial stress increments. If $\Delta\sigma_x/\Delta\sigma_z = K_o$, from Eq. 13 follows:

$$\kappa = \frac{K_o}{1 + K_o} \tag{14}$$

Poisson's ratio computed with Eqs. 9 and 10, results:

$$\nu = \kappa \tan\theta \tag{15}$$

Since the direction of the mean path of the grains in a triaxial compression test (Marsal, 1971), is

$$-\frac{\Delta\varepsilon_r}{\Delta\varepsilon_a} = \cot\theta \tag{16}$$

Then, combining Eqs 15 and 16, one obtains:

$$|\frac{\Delta\varepsilon_r}{\Delta\varepsilon_a}| = \nu = \sqrt{\kappa} \tag{17}$$

The shear modulus G_{TC} for a triaxial compression test can be computed making use of the applied effective stresses and the corresponding principal strains ($G_{TC} = \Delta\tau_{max}/\Delta\gamma = \Delta(\sigma_1-\sigma_3)/2((|\Delta\varepsilon_a| + |\Delta\varepsilon_r|))$. From this expression and Eqs. 9^a to 11^r, it is demonstrated that:

$$\frac{M_{TC}}{G_{TC}} = 2\ (1+\nu) \tag{18}$$

When a soil tested in triaxial compression is unloaded after being stressed to a certain level, the sign of the frictional resistance changes while that of the shear forces remains unaltered; consequently, the modulus of deformation at point A (Fig. 6) has two values (M_{TC} and M'_{TC}), the one for the loading branch being always the smallest; upon reloading a third value M''_{TC} for $\varepsilon_{a,A}$ is obtained and $M''_{TC} > M_{TC}$. The initial tangent moduli at $\varepsilon_{a,o}$ and $\varepsilon_{a,B}$ as well as the hysteresis upon unloading and reloading, depend on the frictional resistance variations caused by the effect of the standard deviations $D(P_{xij})$, $D(P_{yij})$, and $D(P_{zij})$ (see Eq. 3) on the coefficient χ.

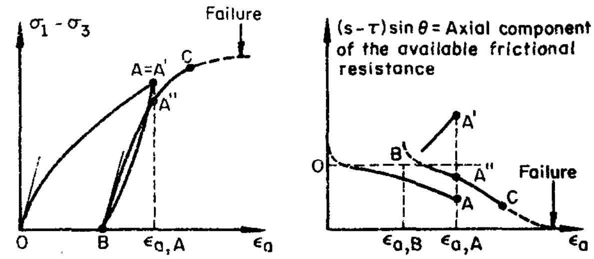

Fig. 6 Variation of the available resistance during a loading cycle in triaxial compression.

Because the available frictional resistance is a vector parallel to the mean path of the particles, the type of the test (e.g., triaxial compression vs plane strain) may have a significant influence, not only on the stress-deformation characteristics, but also on the Mohr's envelope at failure of the soil (Marsal, 1971).

DESCRIPTION OF THE APPARATUS

In order to obtain the basic information required for the statistical theory described previously and test its ability to predict the behavior of granular soils, it was decided to build a device adequate for investigating their deformation characteristics under widely different stress conditions. Also, to complement the previous studies on strength and compressibility of these materials, the device should be capable of handling rockfill samples; consequently, it was anticipated that the specimens should be one cubic meter in volume and include particles up to a nominal diameter of 10cm. These general specifications led to the design of the "true" triaxial apparatus which is described below.

Component parts. As shown in Fig. 7, the space allocated for the specimens is approximately a cube one meter on each side. Its surface is made of a steel sheet 6mm thick, supported by reinforced concrete; this in turn is encompassed by a 10cm thick cast steel cylinder closed by a 15cm base and a cap of variable thickness. The steel container was designed to resist a maximum internal pressure of 100 kg/cm^2.

Normal stresses are applied to the specimen by means of three rubber bags, confined by the walls of the apparatus in the back and a cardboard 1cm-thick in front (Fig. 7). The cardboard not only protects the bag, but also helps in forming the specimen; while placing the material, the lateral cardboards are supported by four movable footing located at the corners of the corresponding specimen face. To avoid interference, the rubber bags are separated by three steel lined, reinforced concrete beams, 20x20cm in cross section. The vertical beam is incorporated into the body of the apparatus and the horizontal ones can be removed.

The rubber bags are the parts that have caused the most trouble. After several trials, a square bag 80cm on each side with round corners, cast and vulcanized in a mold, was adopted.

To minimize the side friction on the specimen, its entire surface is covered with an antifriction lining. This is composed of three layers of greased polystyrene plates, 15x15x0.1cm thick. The plates are glued to soft papers to keep them in proper position while preparing the specimen.

The specimen can be saturated through a porous stone located at the base; at the top, on the vertical beam, a pipe drains off the gas and excess water.

Stress and strains. Stresses are applied to the specimen through the rubber bags which are filled with water. The pressure is produced by three independent hydro-pneumatic pumps that automatically keep constant the state of stress, if required. In order to measure the stresses acting on the three orthogonal axes, the walls opposite to the rubber bags are instrumented with pressure cells of the type used in earth dams (CFE, 1969). Each wall has three pressure cells for detecting arching effects in the specimen. The pressure transmitted to the above cells are registered by means of sets of three electrical Bourdon gages that cover the following pressure ranges: 0-7, 7-28 and 28-100 kg/cm^2. In this manner, the accuracy of the system is $\pm$1.5 percent.

To measure the strains, three electrical extensometers are located adjacent to the fixed walls and they converge at the vertex of the trihedron made by the above walls (Fig. 7). The linear extensometers consist of an end-plate, a steel wire 1mm in diameter, and an electrical potentiometer; the wire is kept in tension with a pair of constant pull springs. To avoid the effect of side friction, the wire is surrounded by telescoping

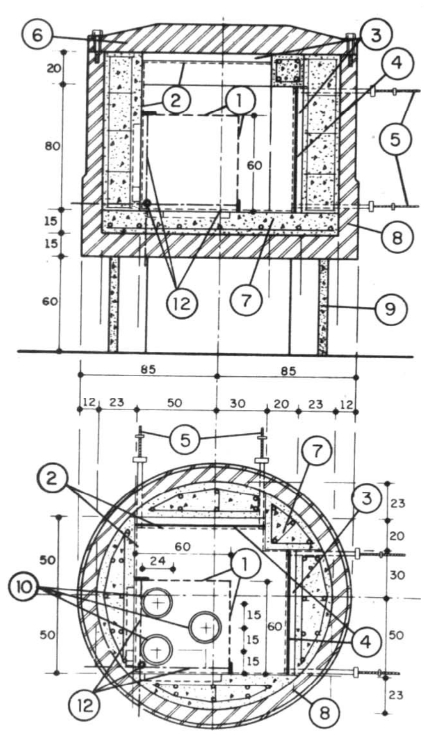

1. Test portion of the specimen
2. Antifriction linings
3. Rubber bags
4. Cardboard
5. Movable footings
6. Steel cap
7. Reinforced concrete
8. Steel cylinder
9. Pedestal
10. Pressure cells
11. Specimen
12. Extensometers
13. Concrete beams
14. Control valves of the pressure cells
15. Hydro-pneumatic pumps
16. Electronic console

Dimensions in centimeters

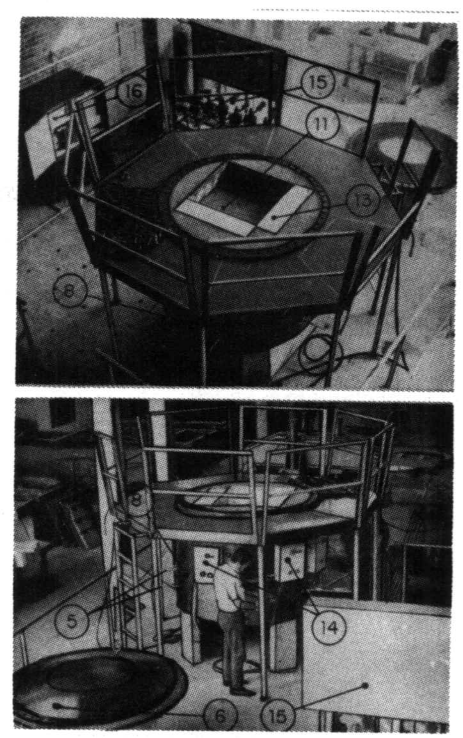

Fig. 7 Vertical and horizontal cross-sections of the "true" triaxial apparatus and photographs of the equipment.

small tubes. Because the vertical and horizontal beams that confine the rubber bags may cause a non uniform state of stress in their vicinity, the initial length of the extensometers is limited to 60cm, so the test portion of the specimen is a cube 60cm on the side. The extensometers read to the nearest millimeter.

Recording of measurements. A data acquisition system is available to convert to punched tape, either automatically or manually, the stress and strain readings during the test. These data will be processed in a computer.

Testing program. At present, the device has been completed and preliminary tests with sand are under way. The specimen is placed in layers 10cm thick, compacted with a vibratory tamper.

In order to determine the values of coefficients a_n and f for different stress levels (including the effect of grain breakage), a series of hydrostatic compression tests will be run. K_0-tests are programmed for finding out the variation of parameter κ with the applied pressure. Finally, triaxial tests will be carried out with various loading cycles and rotation of the principal stress axes.

CONCLUSION

The true triaxial apparatus described in this paper will be used to observe the influence of several factors (e.g., gradation, compaction, loading history, etc.) on the parameters a_n, κ and Q, which are needed for computations with the statistical theory. Although grain breakage was not included in the theoretical developments, the effect of this phenomenon particularly important in rockfills, will be also investigated. Through this comprehensive study, it is expected to improve and simplify the statistical approach to the analysis of the stress-strain behavior of granular soils.

Acknowledgement. The author gratefully acknowledges the valuable help and contribution of Messrs. Luis Ramírez de Arellano and Arturo Núñez G. of the CFE Staff, and of Messrs. Jesús Alberro and Gabriel Auvinet of the Instituto de Ingeniería, UNAM.

REFERENCES

KONDNER, R. L. and ZELASKO, J. S. (1963), "A Hyperbolic Stress-Strain Formulation for Sands", Proc. Second Panamerican Conference on Soil Mechanics and Foundation Engineering, Brazil.

ALBERRO, J. (1971), Análisis y Comportamiento de un Dentellón de Concreto", Proc. Fourth Panamerican Conference on Soil Mechanics and Foundation Engineering, Puerto Rico.

RESENDIZ, D. (1970), "Las Relaciones Esfuerzo-Deformación de los Suelos: una Revisión de Enfoques", Publication of the Institute of Engineering, UNAM, No. 270, Mexico.

MARSAL, R. J. and RAMIREZ DE ARELLANO L. (1967), "Performance of El Infiernillo Dam, 1963-1966", ASCE Journal of the Soil Mechanics and Foundations Division.

MARSAL, R. J. et al. (1965), "Research on the Behavior of Granular Materials and Rockfill Samples", CFE Publication, Mexico.

MARSAL, R. J. (1971), "Suelos Granulares: Modelo Estadístico, Teoría de Falla y Relaciones Esfuerzo-Deformación", Publication of the Institute of Engineering, UNAM, No. 290, Mexico.

MARSAL, R. J. (1963), "Contact Forces in Soils and Rockfill Materials", Proc. Second Panamerican Conference on Soil Mechanics and Foundation Engineering, Brazil.

COMISION FEDERAL DE ELECTRICIDAD (1969), "Notes upon Hydroelectric Works Undertaken in Mexico", CFE Publication, Mexico.

FIELD AND LABORATORY CREEP TESTS ON WEAK ROCKS

ESSAIS DE FLUAGE SUR LES ROCHES FAIBLES

ПОЛЕВЫЕ И ЛАБОРАТОРНЫЕ ИСПЫТАНИЯ ПОЛУСКАЛЬНЫХ ПОРОД НА ПОЛЗУЧЕСТЬ

A.C. MEIGH, Managing Director

B.O. SKIPP, Head of Research, Soil Mechanics Limited, Bracknell, Berkshire

N.B. HOBBS, Director, Rock Mechanics Limited, Bracknell, Berkshire, England

SYNOPSIS. As part of the study of foundation problems associated with heavily loaded structures, such as nuclear power stations, the stress-strain-time behaviour of weak rocks must often be determined. During investigation for the nuclear power station at Heysham, Lancashire, a loading test on a 1.5m diameter plate at 1900 kN/m^2 on a Triassic sandstone was maintained for three months. This paper describes the experimental setup. Observations of the effect of water level changes were made, from which an in-situ value of rock modulus was calculated. The creep behaviour of the plate is compared with laboratory creep tests. In a recent investigation for another nuclear power station at Oldbury, Gloucestershire, to be founded on Triassic sandstones and siltstones, diamond drill core specimens of up to 163 mm diameter were subjected to a triaxial state of stress for periods of up to 700 hrs. This paper describes a new apparatus for this purpose. Examples of creep curves are given their interpretation is discussed, and a simple approach to the prediction of creep settlement is outlined.

INTRODUCTION

Nuclear reactors may with economic advantage be designed to impose high loads on weak rocks. Typically loadings of between 1-2MN/m^2 may be considered on bases from 30m-18m diameter. Such load intensities on weak rocks are not usually encountered in deep foundation practice where there is often some distribution of stress from embedment (piles, shafts) but when imposed by relatively rigid structures on a rock surface without benefit of embedment they approach the classical problem of a rigid punch on a half space, and the dimensions ensure not negligible settlements. Nevertheless the average stresses imposed by such structures are not high when compared with the crushing strength of even weak rocks, 10 MN/m^2.

With structures on rock the greater part of the settlement is expected to be immediate, and, given the construction period, to have been "built out" before operation. Any differential settlements subsequently causing concern would arise from long term strain. There are however major structures for which it is necessary to predict total settlement with some degree of accuracy, and under these circumstances the time settlement component during construction becomes, along with the "immediate" settlement, a factor of engineering significance. This time settlement, called "creep", is defined for engineering purposes as that settlement which follows the immediate settlement and any consolidation settlement occurring on the dissipation of pore pressure.

Two reactor sites on Triassic rocks in England provide the information herein presented, the first at Heysham in Lancashire and the second at Oldbury in Gloucestershire.

CREEP TESTING AT HEYSHAM

The bedrock here is weak to moderately strong (3.0 to 30 MN/m^2) fine to medium grained red sandstone, Bunter Sandstone, of high porosity (15 to 32%). Grains larger than about 200μ are mainly sub-angular to rounded becoming increasingly angular with decreasing size having a fairly high degree of intergranular contact. The cementing matrix is predominantly a red iron oxide probably with clay minerals, although some secondary silica is present. The specimens tested exhibited non-linear elasticity, the secant modulus (0-1.4 MN/m^2) varying between 1400-4200 MN/m^2, with a median value of 2800 MN/m^2 in the drained state. Poisson's Ratio was about 0.1.

Plate Testing

Plate tests (0.6m) were carried out at three levels in a deep shaft primarily to establish a factor between the deformation modulus and the laboratory secant modulus on rock cores. The modulus of deformation (secant 0 to 1.6 MN/m^2) from these plate tests ranged from 550-1400 MN/m^2 with the modulus of elasticity on reloading ranging from 2400-5500 MN/m^2. In these tests four loads were maintained for a duration of 24 hours and indicated that time dependent settlement should be expected.

In view of this it was decided to carry out long-term tests on part of the site where the Bunter Sandstone was nearer the ground surface. A well point system was installed to lower and maintain the ground water at the level of the tests which were carried out in a large shallow excavation on 0.6m and 1.5m diameter plates at two levels, the final 1.5m test being maintained for a period of 117 days. An excavation beneath the position of the final 1.5m diameter plate tests showed the rock to be fairly massive with micaceous bedding surfaces, the apparent bedding dip varying up to 10°, with tight sparse steeply dipping joints under the west side of the plate. At 0.9m below the plate surface, 0.42m of thinly bedded weaker sandstone occurred. Immediately beneath the plate on the east side a thin superficial band of weak material was removed and replaced with mortar.

Load was applied through a 1000 tonne large capacity jack operated manually, the load being measured by a 500 tonne load column. Reaction was provided by deep anchorages grouted into the rock. The datum bar comprised an Invar rod, anchored 9m below the lowest test level, passing through a hole in the plate which consisted of a high strength concrete disc 30 cms thick resting on a 25.4 mm steel plate. The whole loading setup (excluding the reaction beam) and readout system was housed in a double skin thermal cabin with the temperature maintained at 12±1°C.

A study of the effect of small changes in the water level was made by varying the water level below the plate, a linear telation between water level and deformation being derived. The modulus of the rock between the plate and the point of fixity was estimated to be about 1400 MN/m^2 from this relationship. On completion of the temperature and water level studies, a load of 1.9MN/m^2 was applied and maintained for 117 days. After the test had been under way 25 days two of the four dial gauges (reading 10^{-3}in.) were replaced by four arm inductive transducers excited by a 1 kc signal giving a demodulated output via a precision low level switch-box to a pen recorder. A third trans-

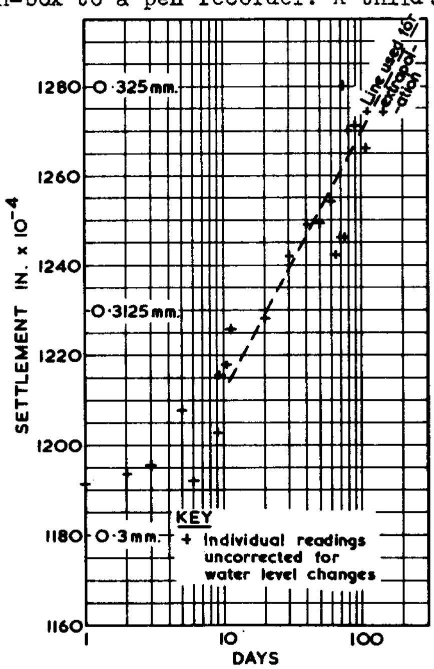

FIG. 2. SETTLEMENT-TIME, 1·5m. PLATE, HEYSHAM

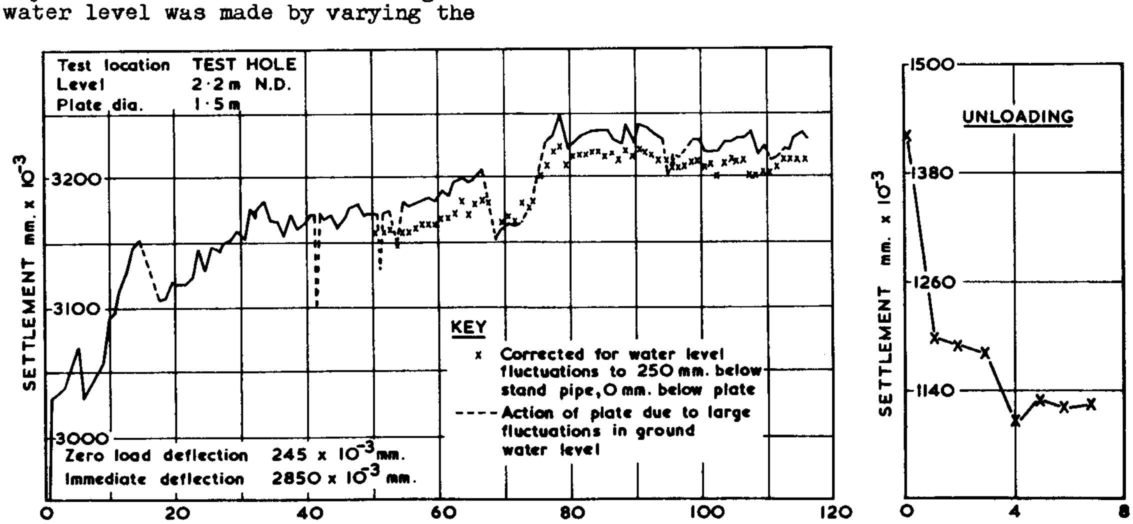

FIG. 1. SETTLEMENT-TIME 1·5m. PLATE, HEYSHAM

ducer was inserted as a dummy to monitor electronic drift. The resolution of the system could be varied, but it was found adequate, in view of background fluctuations in water levels, to maintain it to 12.7×10^{-5}mm per 0.01 millivolt. The settlement and recovery curve is shown in Fig.1 to a natural time scale. The settlement curve was also plotted on semi-log paper, Fig.2, and indicated linearity beyond 10 days. Extrapolation of the rate of creep/time curve (based on a smoothed experimental curve) suggested a terminating state would ensue.

A further extrapolation was made by plotting an averaged rate of creep against time on log-log paper, projecting from various times elapsed from the start of the test and carrying out a step by step integration. In Table I predictions of plate settlements by the various methods together with simple scaling to a 18 m diameter roactor foundation are summarised. A limit calculation was made in which the lowest discernible rate of creep on the plate test was extrapolated linearly to 10,000 hours giving, when scaled to 18.0m diameter, only 15.0 mm of creep settlement.

Extrapolation of Plate Settlement   Table I

Method of Plotting	Creep Settlement Thirty Years mm	
	1.5 m Plate	18m dia. Reactor
Linear-log settlement (all-points)	0.75	10.5
Log creep rate-log time (elapsed time thirty-five days)	0.65	7.5
Log creep rate-log time (elapsed time seventy-five days)	0.28	3.5
Log creep rate-log time (elapsed time ninety days)	0.25	3.3

Laboratory Creep Testing

Unconfined creep tests were carried out on 10 specimens with stresses generally maintained within the range of values shown in Table II for up to 1000 hrs. Most tests were made on a lever arm/dead weight frame but several were carried out with the hydraulic/screw frame developed for concrete testing by the C.E.B.T.P.(Paris). With this apparatus it was only possible to start strain measurements after application of the load. A few triaxial tests were also carried out. The results in the form of strain versus log time are given in Fig.3. It was noted that the modulus of elasticity based on the strain measured at as short a time after loading as possible was lower than the average secant modulus obtained from standard tests on generally larger specimens.

Comparison of Plate and Laboratory Tests

The plate may be regarded as a rigid punch upon a linear viscoelastic half space for which a solution may be developed at small strains and in the absence of body forces by using the correspondence principle between the elastic constants and the viscoelastic operators describing deviatoric and dilatational relations between stress and strain. A full solution would require knowledge of both deviatoric and volumetric time strain behaviour. The determination of the necessary rheological parameters is both difficult and expensive, and in any case the values obtained in the laboratory on small samples would be of doubtful applicability, therefore a simple relationship was sought between the modulus of elasticity of the rock "skeleton" and the subsequent creep strain. The consolidation during the dissipation of pore pressure may be regarded as a hydrodynamic "delay" and the rate of stress application reduced accordingly in order to obtain the skeleton or drained modulus of the rock. At Heysham the high fabric permeability (10^{-5}m/sec) ensured that the moduli measured were in fact "drained". The creep index may be regarded as the creep settlement per log cycle expressed as a proportion of the immediate settlement (Burland, 1970) or as the creep settlement contribution extrapolated to some convenient date, say, the life of the structure. One may then use, as a factor reducing the short term modulus, the ratio between the secant modulus shortly after loading a specimen, but on completion of pore pressure dissipation, and the secant modulus at a strain at the postulated life of the structure. The predicted settlement of the plate, or the foundation on an elastic basis can then be easily adjusted to allow for any creep. Values of this reduction factor established by graphical extrapolation of the laboratory creep curves and those obtained by comparing the short term settlement of the plate with the settlement predicted for 30 years are given in Table II.

With the linear viscoelastic model it is permissible to scale directly from the plate test to the full reactor diameter with respect to total settlement at the chosen time and to the rate of settlement. Alternatively the "reduction factor" deduced from the plate test may be applied to the estimate of short term "elastic settlement of the foundation made on the basis of the modulus profile assessed from consideration of the deep plate loading tests, laboratory tests on cored specimens, and other in-situ tests such as the Menard pressuremeter, and also taking account of the drill logs.

For one condition studied, a 18 m diameter reactor applying a gross pressure of $1.9 MN/m^2$, short term settlements of 22mm were predicted with an additional creep settlement of 12mm using a reduction factor of 0.65. By simple extrapolation of the short term settlement of the 1.5m diameter plate to the same reactor dimensions and loading, a short term settlement of 25mm was predicted with an additional creep settlement of 11 mm.

Short and Long Term Modulus Test Results Table II

Sample No.	Deviator Stress 1 - 3 KN/m^2	Cell Pressure 3 KN/m^2	Diameter mm	Secant Modulus: Short term E_i MN/m^2	Secant Modulus: Long term E_r (MN/m^2)	E_r/E_i
30	1760	-	5.1	380	240	0.63
31	1760	-	5.1	1560	1030	0.66
53a	880	1030	2.54	180	130	0.72
53b	880	-	2.54	160	130	0.81
70b	860	1030	2.54	340	300	0.88
168	1800	-	5.1	540	490	0.91
169	1800	-	5.1	470	380	0.81
PLATE				740	580	0.79

The general validity of the above approach may be qualified by a number of special circumstances; the sandstone is porous and permeable, the value of Poisson's Ratio is low. Stresses were estimated as "average" under the foundation and the effect of stress level on creep rate was not established, as the applied stresses were small compared with the strength of the rock.

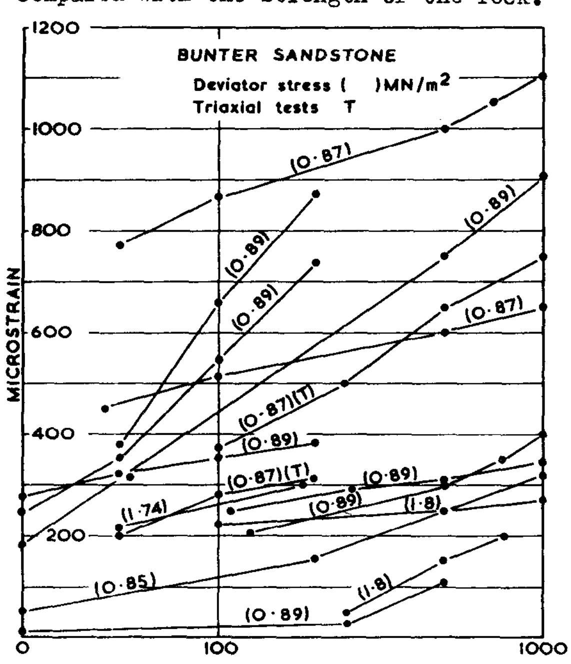

FIG. 3. LABORATORY CREEP CURVES, HEYSHAM

CREEP MEASUREMENTS AT OLDBURY

During 1970-71 the investigations for a proposed nuclear power station at Oldbury, Gloucestershire, creep testing could only be carried out in the laboratory because difficult ground water conditions precluded plate tests.

At Oldbury a variegated sequence of Triassic siltstones and sandstones is underlain by Devonian sandstones and mudstones. In the upper 15m of the Triassic (Keuper) the sandstones are characterised by cavities from which gypsum has been removed. The sequence is difficult to sample with normal diameter tools so large diameter coring was used to recover 163 mm diameter specimens.

The type of creep test was chosen to simulate as closely as possible the stress state to which the test specimens would be subjected under the reactor foundation. Thus the weaker siltstones at the upper levels were tested in either conventional oedometers or flexible loading "Rowe" cells (Rowe & Barden, 1966) while the stronger and more open jointed sandstones were tested in lever arm frames without confining pressure. Intermediate materials were tested triaxially, and in order to accommodate the 163mm diameter specimens special triaxial cells had to be constructed.

Large Diameter Triaxial Creep Cells

The cell consists of high pressure steel pipe having an internal diameter of 300 mm and length of 700mm fitted with robust end plates, the lower plate carrying the specimen pedestal. The cell is designed to withstand a pressure of 3 MN/m^2.

Axial loading of the specimen is by a flexible diaphragm supported by a plate 3mm smaller in diameter than the bore of the cell. Electrical and pressure services apart from the pressure line supplying axial load enter through the base. A diagram showing the cell and pressure system is given in Fig.4.